

## INFLUENCE OF NICKEL ON STRUCTURAL AND OPTICAL BEHAVIOUR OF CADMIUM SULPHIDE NANOPARTICLES

K. P. TIWARY<sup>a,\*</sup>, F. ALI<sup>b</sup>, R. K. MISHRA<sup>c</sup>, S. K. CHOUBEY<sup>d</sup>, K. SHARMA<sup>e</sup>,  
*<sup>a</sup>Department of Physics, Birla Institute of Technology Mesra, Patna Campus,  
Patna-800014, India*

*<sup>b</sup>Centre for Nanoscience and Nanotechnology, Jamia Millia Islamia, New Delhi-  
110025, India*

*<sup>c</sup>Department of Electrical and Electronics Engineering, Birla Institute of  
Technology Mesra, Patna Campus, Patna-800014, India*

*<sup>d</sup>Department of Electronics and communication Engineering, Birla Institute of  
Technology Mesra, Patna Campus, Patna-800014, India*

*<sup>e</sup>Department of Chemistry, Birla Institute of Technology Mesra, Patna Campus,  
Patna-800014, India*

Cadmium Sulphide being an important II-VI compound semiconductor has wide applications in various optoelectronic and biolabeling devices. In the present work, undoped and Ni (2%, 4%, 6% and 8%) doped CdS nanoparticles were synthesized in aqueous medium by microwave assisted solvo thermal method using cadmium acetate, nickel chloride and sodium sulphide as precursors. The effect of Ni doping on the Structural, Morphological and Optical Properties of CdS nanoparticles have been studied by X- ray diffraction, SEM, FTIR, PL and UV-Visible spectroscopy. The crystal structure and morphology of the as synthesized nanoparticles have been investigated by X- ray diffraction and scanning electron microscopy (SEM). The XRD results revealed the crystalline nature of the nanoparticles. The average grain size of the nanoparticles was estimated using Scherrer equation which was found to be in the range of 4.2 - 6 nm. The FTIR spectra were also recorded to identify the presence of various functional groups in the synthesized CdS nanoparticles. For the estimation of the optical energy band gap of as synthesized nanoparticles, absorption spectra were recorded using UV- Visible spectrophotometer. The result of UV-Visible spectra revealed the increment of energy band gap in CdS nanoparticles on increasing the concentration of Ni.

(Received May 12, 2020; Accepted August 27, 2020)

*Keywords:* Ni doped CdS nanoparticles, XRD, SEM, FTIR, Photoluminescence

### 1. Introduction

In the recent past, II-VI compound semiconducting nanoparticles have attracted a great deal of attention due the quantum confinement effects imparting peculiar properties as compared to their bulk crystals[1-2]. The binary compound semiconductors are prominent material for the fabrication of various biolabeling and drug delivery system as well as optoelectronic devices like light photoconductive cells, laser diodes (LDs), LEDs, memory device, solar cells, etc [3-9]. Among II-IV compound semiconductor, CdS is chemically more stable as compared to other chalcogenides, which makes it a perfect host material having wide application in optoelectronics [10-12]. The low energy bandgap enables it to be used as window in solar cells [13-14]. Therefore, doping of CdS with any transition metal (like Cr, Fe, Co, Ni, Cu, Zn, etc) is essential for such kind of applications [15-21].

Among these transition metals, Ni impurities are considered as perfect acceptor in CdS, which tunes its structural and optical properties [22-23]. The various approaches for the synthesis of CdS nanoparticles includes sol gel technique, chemical co- precipitation, spray pyrolysis,

---

\* Corresponding author: kptiwary@bitmesra.ac.in

solvothermal, microwave (MW) assisted synthesis, etc [24-29]. As we know that nanoparticles have very high surface to volume ratio due to which CdS at nanosize attains high surface energy therefore it is a sophisticated task to precise the growth of nanosized CdS [30]. Repeated heating and cooling in microwave oven may control the unwanted growth of CdS particles and hence can be limited within the range of nanoparticle size [26-27, 31]. In this work, we have selected microwave (MW) assisted method for the synthesis of undoped and Ni doped CdS nanoparticles and detailed investigation of structural, morphological and optical properties has been discussed. Further this study reveals the size dependence of energy bandgap of the synthesized nanoparticles.

## **2. Experimental**

### **2.1. Chemicals**

The glassware used for the experimental work were washed with acid and dried to avoid the impurities before using it for the synthesis process. The following materials were used for the synthesis of undoped and Ni doped CdS. Double distilled water was used for all dilution and sample preparation. Cadmium acetate ( $\text{Cd}(\text{CH}_3\text{COO})_2 \cdot 2\text{H}_2\text{O}$ ), nickel chloride ( $\text{NiCl}_2$ ) and sodium sulphide ( $\text{Na}_2\text{S} \cdot x\text{H}_2\text{O}$ ) obtained from Molychem were used as precursors. The chemical reagents used were of analytical grade and were used without further purification.

### **2.2. Synthesis**

The synthesis of undoped and Ni doped CdS nanoparticles was carried out in aqueous medium using Microwave assisted solvo thermal method. In a typical experiment, for the synthesis of undoped CdS nanoparticles, aqueous solution of cadmium acetate ( $\text{Cd}(\text{CH}_3\text{COOH})_2 \cdot 2\text{H}_2\text{O}$ ) and sodium sulphide ( $\text{Na}_2\text{S}$ ) were prepared and combined stoichiometrically. The solution was stirred for 30 minutes at room temperature to make the solution homogeneous and followed by microwave process. The microwave process involved microwave irradiation of the solution for 20 seconds and then relaxed for the next 60 seconds making a complete cycle with 25 % duty cycle. About 15 cycles took for the formation of CdS nanoparticles. The obtained yellowish colloidal solution containing CdS nanoparticles was separated centrifugally and washed properly several times. The obtained residue was dried in oven for 10 hours at 70° C and finally moisture free undoped CdS nanoparticles were obtained. Similarly, for synthesis of Ni doped CdS nanoparticles, aqueous solution of cadmium acetate and required amount of nickel chloride were combined stoichiometrically and stirred for 30 minutes at room temperature. The concentration of the Ni was adjusted in the solution for varying the doping concentration of Ni in the following manner i.e. 2 %, 4%, 6% and 8%. Post stirring process, aqueous solution of sodium sulfide was added in a drop wise manner to the above mixture. The above mentioned microwave process followed by centrifugation and drying of sample in oven was repeated for obtaining Ni (2 %, 4%, 6% and 8%) doped CdS nanoparticles.

### **2.3. Characterization techniques**

The as synthesized nanoparticles were examined using following techniques: The X-ray diffraction (XRD) spectra of the samples were recorded using X-ray diffractometer (RIGAKU) with a Cu  $k\alpha$  radiation ( $\lambda=1.54060$  Angstrom) for investigating the structural property. The average crystallite size was estimated using Scherer equation  $(0.9\lambda)/(\beta \cos\theta)$  at the full width half maximum of XRD peaks. The morphology of nanoparticles was examined using scanning electron microscope (SEM; JEOL-JSM-6390 LV). FTIR spectra were recorded using FTIR spectrometer (SHIMADZU-IR-Prestige 21) for identification of various functional groups present in the nanoparticles. The study of optical properties of the prepared samples of CdS at varying doping concentration of nickel was done by Photoluminescence (SHIMADZU-RF-5301PC), and UV-visible (RAYLEIGH UV 2601) spectra, recorded at room temperature.

### 3. Results and discussion

#### 3.1. XRD studies

The structural properties of the prepared Ni doped CdS nanoparticles have been examined by XRD analysis. The X-ray diffraction provides the information regarding the crystalline structure and average grain size of the nanoparticles. The X-ray diffraction spectra of the prepared undoped and Ni (2%, 4%, 6% and 8%) doped CdS nanoparticles are shown in figure 1(a-e). The XRD spectra revealed that the as synthesized CdS nanoparticles has three major peaks, observed at diffraction angle  $26.5^\circ$ ,  $44^\circ$  and  $51.5^\circ$  corresponding to (111), (220) and (311) planes respectively. No major changes were observed in the peak position of Ni doped CdS with respect to that of undoped CdS.

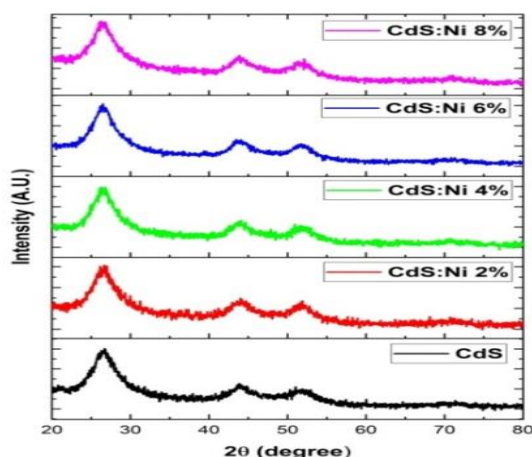


Fig. 1. XRD spectra of Ni doped CdS nanoparticles.

The obtained XRD pattern of the nanoparticles matches well with the standard cubic CdS (JCPDS Card No. 10 - 454). The nanosize of the prepared particles of undoped and Ni doped CdS has been clearly indicated by the broadening of the diffraction peaks. The average crystallite size has been determined using Scherrer equation:

$$D = \frac{k\lambda}{\beta \cos\theta} \quad (1)$$

where,  $k$  is shape factor of particle (generally taken as 0.9),  $\lambda$  is the wavelength of X-ray source ( $1.54060 \text{ \AA}$ ),  $\beta$  is Full Width at Half Maximum value and  $\theta$  is the diffraction angle. The average crystallite size of Ni (0%, 2%, 4%, 6% and 8%) doped CdS was found to be around 5.13 nm, 4.79 nm, 4.68 nm, 4.47 nm and 4.27 nm respectively. The inter planer spacing has been calculated via Bragg's law:

$$n\lambda = 2d \sin\theta \quad (2)$$

In equation (2),  $n$  is the order of diffraction,  $d$  is the inter planer spacing and  $\lambda$  and  $\theta$  have the usual meanings. The values of  $d$  were found to be slightly decreased from 0.343 nm (for undoped CdS) to slightly lower values for the increased concentration of Ni. This may be due to the smaller ionic radius of Ni ( $0.72 \text{ \AA}$ ) as compared to that of Cadmium ion ( $0.97 \text{ \AA}$ ). Lattice constant may be calculated using equation (3).

$$d = a / (h^2 + k^2 + l^2)^{1/2} \quad (3)$$

By substituting the value of  $d$  in equation (3), the corresponding value of lattice constant ( $a$ ) can be calculated and hence volume of unit cell can be calculated from the following relation given in equation (4). The variation in average crystallite size ( $D$ ), Interplanar spacing ( $d$ ), Lattice constant ( $a$ ), volume of Unit cell ( $a^3$ ) and optical energy band gap ( $E_g$ ) of undoped and Ni doped CdS nanoparticles are given in Table 1.

$$V = a^3 \quad (4)$$

### 3.2. SEM studies

The surface morphology of the prepared Ni doped CdS nanoparticles have been examined using SEM analysis. Fig. 2 (a-c) illustrates the obtained SEM micrograph of the synthesized CdS nanoparticles at varying doping concentration of Ni (6% and 8%).

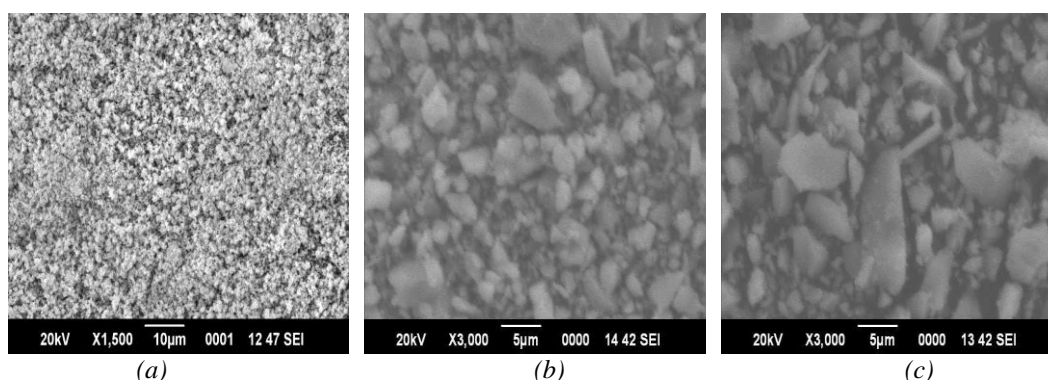


Fig. 2 (a-c). SEM image of undoped and Ni (6% and 8%) doped CdS nanoparticles respectively.

The micrograph clearly indicates that the nanoparticles have smooth surface and appears to be roughly spherical in shape. The nanoparticles seem to be highly agglomerated which might be due to the absence of capping agent in the prepared solution during the synthesis. The obtained SEM micrograph shows considerable change in morphology and porosity of the prepared CdS nanoparticles on doping it with Ni.

### 3.3. FTIR studies

The various vibrational and functional groups present in the prepared Ni doped CdS nanoparticles were investigated by FTIR spectra analysis. Figure 3(a-e) illustrates the FTIR spectra of the synthesized CdS nanoparticles.

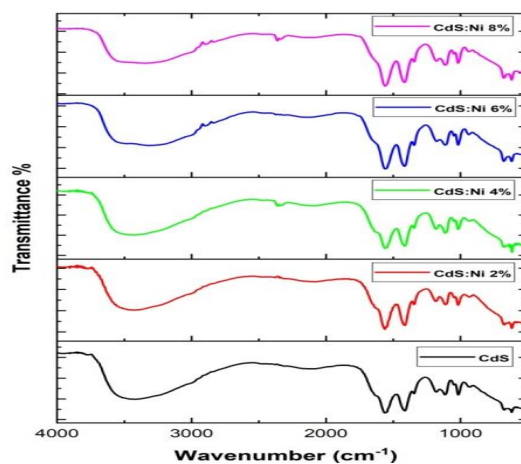


Fig. 3. FTIR spectra of Ni doped CdS nanoparticles

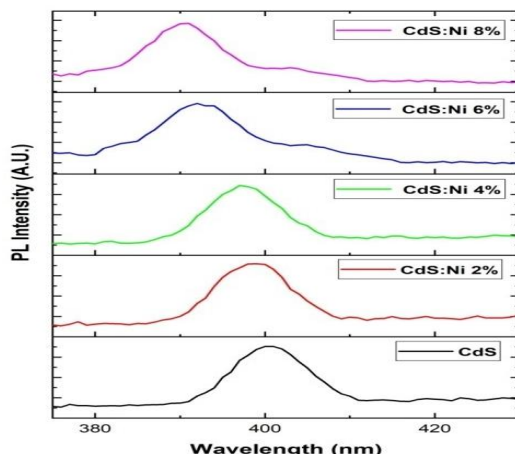


Fig. 4. PL spectra of Ni doped CdS nanoparticles.

All the samples have been analyzed in the range of  $4000\text{-}500\text{ cm}^{-1}$  at room temperature. The broader and weak absorption band around  $3400\text{-}3600\text{ cm}^{-1}$  has been assigned to OH stretching. The absorption peak around  $2800\text{-}2900\text{ cm}^{-1}$  has been assigned to C-H stretching. The weak peaks observed in the range of  $2100\text{-}2300\text{ cm}^{-1}$  are assigned to  $\text{CO}_2$  molecules. The sharp peak around  $1560\text{ cm}^{-1}$  indicates the presence of H-O-H bending vibration of water molecules, which indicates the presence of moisture in the sample. The small sharp peaks in the range of  $1000\text{-}1150\text{ cm}^{-1}$  are possibly due to sulphate group stretching vibrations. The sharp peak around  $617\text{-}627\text{ cm}^{-1}$  corresponds to Cd-S stretching. It is clearly seen from the figure that there is no major shift in Cd-S bond after Ni is doped. Ni incorporation as well as size effect may be responsible for the observed minor shift in the frequency when compared with undoped Cd-S bond.

### 3.4. Photoluminescence (PL) studies

The luminescence properties of the prepared nanoparticles were studied using photoluminescence spectra, recorded at room temperature with excitation  $\lambda = 340\text{ nm}$  having Xenon light source. Fig. 4 shows the PL spectra of CdS nanoparticles at different doping concentration of Ni, obtained at the excitation wavelength of  $340\text{ nm}$ .

The emission bands are observed at  $400\text{ nm}$ ,  $398\text{ nm}$ ,  $396\text{ nm}$ ,  $392\text{ nm}$  and  $390\text{ nm}$  for  $0\%$ ,  $2\%$ ,  $4\%$ ,  $6\%$  and  $8\%$  Ni doped CdS respectively. Blue shift emissions in the prepared CdS nanoparticles have been clearly observed from the figure. The enhancement of band gap with the variation of dopant is clearly indicated by the shifting of emission spectra towards left. The blue shift observed in the spectra might be due to the exhibition quantum confinement effect by the CdS nanoparticles. The position of emission peak shifts towards higher energy with the decrease of nanoparticles size.

### 3.5. UV- Visible

The optical absorption spectra of the synthesized nanoparticles were studied using UV-Visible spectrophotometer from  $200\text{ nm}$  to  $800\text{ nm}$  at room temperature. The absorption spectra of undoped and Ni doped CdS nanoparticles is shown in figure 5(a-e). The figure of absorption spectra clearly indicates the blue shift after doping of Ni in CdS.

The optical energy bandgap of the synthesized nanoparticles were calculated via Tauc equation, which is given by:

$$\alpha h\nu = A (h\nu - E_g)^n \quad (5)$$

where  $\alpha$  is the absorbance,  $A$  is a constant,  $h\nu$  represents the energy of incident photon,  $E_g$  is the energy bandgap value of the sample, and the value of  $n$  can be  $1/2$ ,  $2$ ,  $3/2$ , etc depending on the type of transitions. The value of  $n$  is taken to be  $1/2$ , since this is the case of direct bandgap.

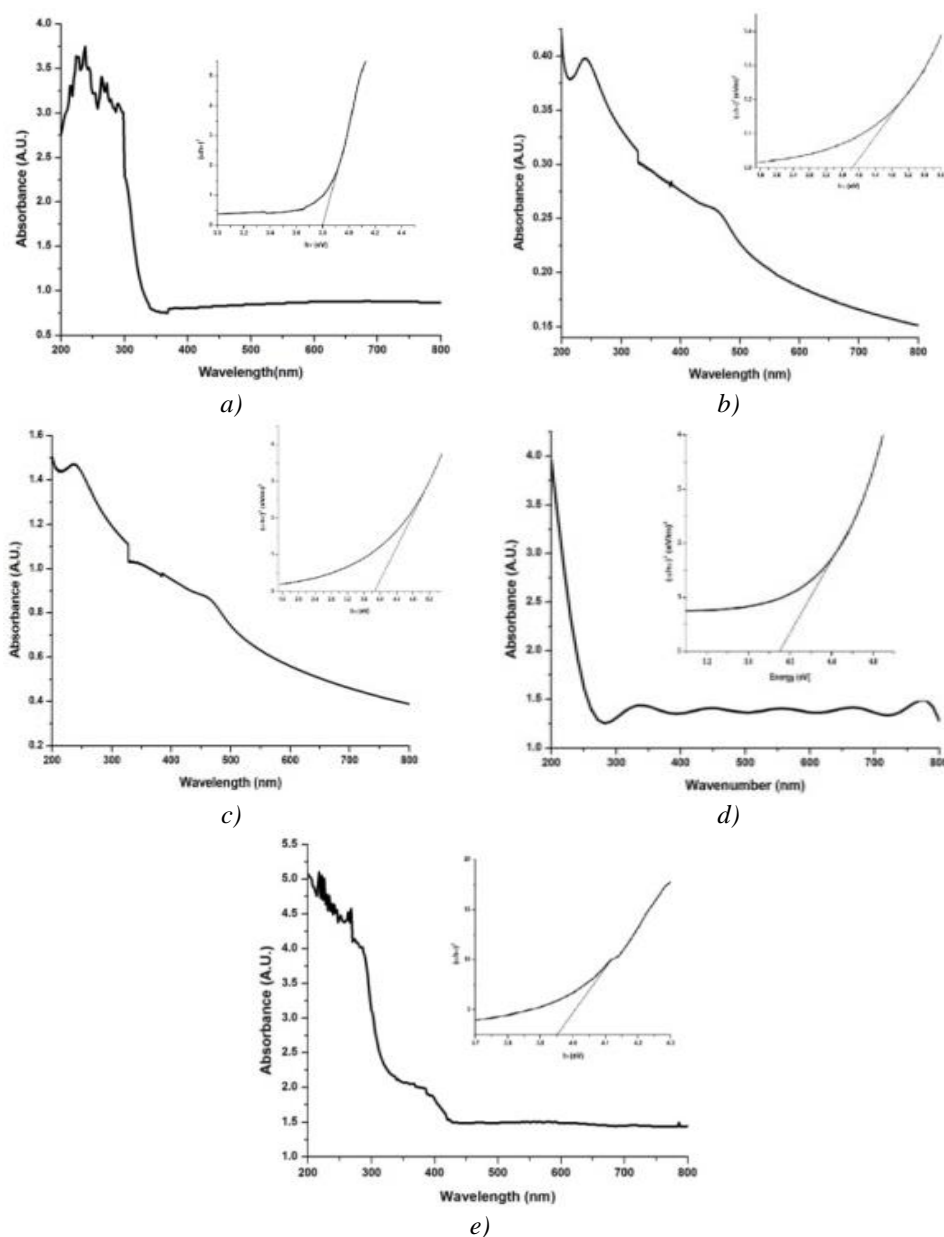


Fig. 5( a-e). Absorption spectra and energy band gap of Ni (0%, 2%, 4%, 6% and 8%) doped CdS nanoparticles.

The energy bandgap ( $E_g$ ) has been estimated via plotting the graph of  $(\alpha h\nu)^2$  versus  $h\nu$  as shown in the Fig. 5(a-e). The extrapolation of the straight line of  $(\alpha h\nu)^2$  to the  $h\nu$  axis gives the energy bandgap value (in eV) of the synthesized CdS nanoparticles. The optical bandgap of undoped CdS is found to be 3.8 eV and 2%, 4%, 6% and 8% Ni doped CdS, it is found to be 3.83 eV, 3.87 eV, 3.90 eV and 3.94 eV respectively which is shown in Fig. 6.

It can be clearly seen from the figure that the optical energy bandgap of Ni doped CdS increases with the increased doping concentration of Ni.

Table 1. Variation of Ni concentration, average crystallite size ( $D$ ), Interplanar spacing ( $d$ ), Lattice constant ( $a$ ), volume of Unit cell ( $a^3$ ) and optical energy band gap ( $E_g$ ) of undoped and Ni doped CdS nanoparticles.

Compound	Avg. crystallite size (nm)	Interplanar Spacing 'd' (Å)	Lattice Constant 'a' (Å)	Volume of unit cell 'a <sup>3</sup> ' (Å) <sup>3</sup>	Optical energy band gap ( $E_g$ ) (eV)
CdS	5.13	3.45	5.98	214	3.80
CdS:Ni 2%	4.79	3.40	5.88	203	3.83
CdS:Ni 4%	4.68	3.38	5.85	200	3.87
CdS:Ni 6%	4.47	3.36	5.82	197	3.90
CdS:Ni 8%	4.27	3.34	5.78	193	3.94

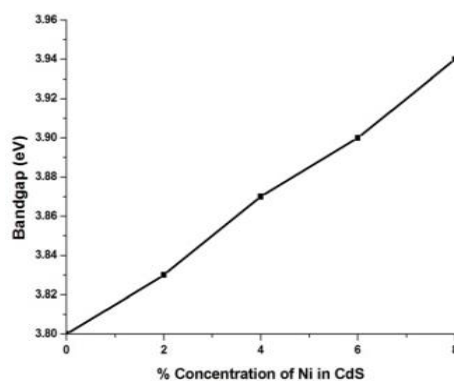


Fig. 6. Variation of Bandgap with doping concentration of Ni in CdS.

Hence, blue shift is observed, which may be due to quantum confinement effect. Figure 6 illustrate the increase in bandgap with the increasing concentration of Ni in CdS.

#### 4. Conclusions

Undoped and Ni doped CdS are among those II-VI semiconductors, which are prominent candidate for the various biological applications like medical diagnosis and drug delivery as well as optoelectronic devices applications like, solar cells, which has been studied in the present work. Microwave assisted method was used for successful synthesis of undoped and Ni doped CdS nanoparticles. The cubic structures of the as synthesized particles were confirmed by XRD analysis. The average crystallite size of undoped and Ni (2%, 4%, 6% and 8%) doped CdS was found to be 5.13 nm, 4.79 nm, 4.68 nm, 4.47 nm and 4.27 nm respectively. The XRD results clearly indicate the decrease in the average crystallites size with the increase in dopant concentration in CdS. The SEM micrograph indicates the prepared CdS particles are spherical and it shows agglomeration.

The different functional groups present on the surface of CdS nanoparticles were identified using FTIR spectra. PL emission peaks were observed in the range 390 nm – 400 nm. Slight blue shift in the emission peaks were observed with the increase in the dopant (Nickel) concentration. The optical energy band gap was observed from UV-Visible spectra and was found to be about 3.80 eV, 3.83 eV, 3.87 eV, 3.90 eV and 3.94 eV for undoped, Ni (2%, 4%, 6% and 8%) doped CdS nanoparticles respectively. UV Visible spectra show that the band gap of CdS nanoparticles is slightly increasing with the increasing doping concentration of Ni

### Acknowledgements

The authors would like to extend gratitude to Central Instrumentation Facility, BIT Mesra, for providing XRD, SEM, PL and FTIR facilities and also to the Department of Chemistry, BIT Patna for providing the UV-Visible spectroscopy facility.

### References

- [1] P. A. Chate, S. S. Patil, J. S. Patil, D. J. Sathe, P. P. Hankare, *Phys. B* **411**, 118 (2013).
- [2] S. Abdulwahab, Z. Lahewil, Y. Al-Douri, U. Hashim, N. M. Ahmed, *Sol. Energy* **86**(11), 3234 (2012).
- [3] S. K. Choubey, A. Kaushik, K. P. Tiwary, *Chalcogenide Letters* **15**(3), 125 (2018).
- [4] Y. Gu, E. S. Kwak, J. L. Lensch, J. E. Allen, T. W. Odom, L. J. Lauhon, *Applied Physics Letters* **87**(4), 043111 (2005).
- [5] S. K. Choubey, A. Kaushik, K. P. Tiwary, *Materials Today: Proceed.* **21**, 1943 (2020).
- [6] L. S. S. Singh, K. P. Tiwary, R. K. Purohit, Z. H. Zaidi, M. Husain, *Current Appl. Phys.* **5**(4), 351 (2005).
- [7] A. A. Ibiyemi, A. O. Awodugba, O. Akinrinola, A. A. Faremi, *J. Semiconduct.* **38**, 093002 (2017).
- [8] K. P. Tiwary, H. Abbas, L. S. S. Singh, M. Husain, *Materials Science in Semiconductor Processing* **13**(2), 102 (2010).
- [9] K. P. Tiwary, S. K. Sinha, S. A. Khan, L. S. S. Singh, M. Husain, Z. H. Zaidi, *Chalcogenide Lett.* **5**(12), 309 (2008).
- [10] R. Seoudi, A. A. Shabaka, M. Kamal, E. M. Abdelrazek, *Physica E* **45**, 47 (2012).
- [11] W. Q. Peng, G. W. Cong, S. C. Qu, Z. G. Wang, *Optical Materials* **29**(2), 313 (2006).
- [12] A. Pan, H. Yang, R. Yu, B. Zou, *Nanotechnology* **17**(4), 1083 (2006).
- [13] V. Singh, P. K. Sharma, P. Chauhan, *Materials Characterization* **62**(1), 43 (2011).
- [14] S. Chavhan, R. P. Sharma, *J. Phys. Chem. Solids* **66**(10), 1721 (2005).
- [15] S. Kumar, S. Rajpal, S.K. Sharma, D. Roy, S.R. Kumar, *Journal of Ovonic Research*, **14**(3), 185 (2018).
- [16] M. Elango, D. Nataraj, K. Prem Nazeer, M. Thamilselvan, *Materials Research Bulletin* **47**(6), 1533 (2012).
- [17] Nikita H. Patel, M. P. Deshpande, S. H. Chaki, *Materials Science in Semiconductor Processing* **31**, 272 (2015).
- [18] M. Muthusamy, S. Muthukumaran, *Optik* **126**(24), 5200 (2015).
- [19] P. Chand, R. Ghosh, Sukriti, *Optik* **161**, 44 (2018).
- [20] K. P. Tiwary, K. Sharma, Neha Bala, Firdaus Ali, *Materials Today: Proceed.* **18**, 1380 (2019).
- [21] K. P. Tiwary, F. Ali, R. K. Mishra, S. Kumar, K. Sharma, *Digest Journal of Nanomaterials and Biostructures* **14**(2), 305 (2019).
- [22] Y. Kashiwaba, K. Isojima, K. Ohta, *Solar energy materials and solar cells* **75**(1-2), 253 (2003).
- [23] K. Siva Kumar, A. Divya, P. Sreedhara Reddy, *Applied Surface Science* **257**(22), 9515 (2011).
- [24] Hadeel Salih Mahdi, Azra Parveen, Shraddha Agrawal, Ameer Azam, *AIP Conference Proceedings* **1832**, 050012 (2017).
- [25] A. Mercy, A. Jesper Anandhi, K. Sakthi Murugesan, R. Jayavel, R. Kanagadurai, B. Milton Boaz, *Journal of Alloys and Compounds* **593**, 213 (2014).
- [26] I. A. Lopez, A. Vazquez, I. Gomez, *Revista Mexicana de Fisica* **59**(2), 160 (2013).
- [27] S. K. Choubey, K. P. Tiwary, *Digest Journal of Nanomaterials and Biostructures* **11**(1), 33 (2016).
- [28] A. Rmili, F. Ouachtari, A. Bouaoud, A. Louardi, T. Chtouki, B. Elidrissi, H. Erguig, *J. Alloys Compd.* **557**, 53 (2013).
- [29] Shiv Kumar Choubey, K. P. Tiwary, *International journal of Innovative Research in science*,

- Engineering and Technology **3**(3), 10670 (2014).
- [30] Y. Al-Douri, A. H. Reshak, *Optik* **126**(24), 5109 (2015).
- [31] K. P. Tiwary, S. K. Choubey, K. Sharma, *Chalcogenide Letters* **10**(9), 319 (2013).